Biochemical and Biophysical Research Communications 430 (2013) 1–6

Contents lists available at SciVerse ScienceDirect

Biochemical and Biophysical Research Communications

journal homepage: www.elsevier.com/locate/ybbrc

Model membrane interaction and DNA-binding of antimicrobial peptide Lasioglossin II derived from bee venom

Susmita Bandyopadhyay [a], Meryl Lee [a], J. Sivaraman [b], Chiradip Chatterjee [a,*]

[a] School of Applied Sciences, Republic Polytechnic, Singapore
[b] Department of Biological Sciences, National University of Singapore, Singapore

ARTICLE INFO

Article history:
Received 29 October 2012
Available online 14 November 2012

Keywords:
Antimicrobial peptide
Lasioglossin II
Micelle
DPC
CD
NMR
pUC19 DNA

ABSTRACT

Lasioglossins, a new family of antimicrobial peptide, have been shown to have strong antimicrobial activity with low haemo-lytic and mast cell degranulation activity, and exhibit cytotoxic activity against various cancer cells *in vitro*. In order to understand the active conformation of these pentadecapeptides in membranes, we have studied the interaction of Lasioglossin II (LL-II), one of the members of Lasioglossins family with membrane mimetic micelle Dodecylphosphocholine (DPC) by fluorescence, Circular Dichroism (CD) and two dimensional (2D) ^{1}H NMR spectroscopy. Fluorescence experiments provide evidence of interaction of the N-terminal tryptophan residue of LL-II with the hydrophobic core of DPC micelle. CD results show an extended chain conformation of LL-II in water which is converted to a partial helical conformation in the presence of DPC micelle. Moreover we have determined the first three-dimensional NMR structure of LL-II bound to DPC micelle with rmsd of 0.36 Å. The solution structure of LL-II shows hydrophobic and hydrophilic core formation in peptide pointing towards different direction in the presence of DPC. This amphipathic structure may allow this peptide to penetrate deeply into the interfacial region of negatively charged membranes and leading to local membrane destabilization. Further we have elucidated the DNA binding ability of LL-II by agarose gel retardation and fluorescence quenching experiments.

1. Introduction

Antimicrobial resistance (AMR) is a global concern for treatment of infectious diseases in recent years. Infections caused by resistant microorganisms often fail to respond to conventional treatment, resulting in prolonged illness and greater risk of death (ref). To treat infections caused by multidrug-resistant microorganisms, searching for new antibiotics has become inevitable and urgent which has stimulated interest in the development of anti microbial peptides (AMPs) as human therapeutics [1].

Naturally occurring AMPs represent one of the first evolved and successful forms of chemical defense of eukaryotic cells against bacteria, protozoa, fungi, and viruses [2]. Unlike currently available conventional antibiotics, which typically interact with a specific target protein, most of these cationic AMPs target the cell membrane of invading microorganisms and leading to cell lyses and death [3,4]. Thus, AMPs offer the possibility of a new class of therapeutic agents, which are complementary to existing antibiotics, and to which bacteria may not be able to develop resistance.

In addition to antibacterial and anti viral activities of AMPs, recent studies show evidences on anticancer activities of some AMPs as well [5]. Though it is believed that the electrostatic attraction between the negatively charged components of bacterial and cancer cells and the positively charged AMPs play a major role in the strong binding and selective disruption of bacterial and cancer cell membranes, respectively. It is not clear whether the molecular mechanism(s) underlying the antibacterial and anticancer activities of AMPs are the same or different. While in most of the cases the bactericidal activity of AMPs is due to the disruption of the membrane integrity *via* various mechanisms that lead to leakage of ions and metabolites, there are reports where AMPs interact with intracellular targets like DNA in bacteria with or without disrupting the cell membrane [6]. AMPs having the ability to interact with double stranded DNA under physiological condition may show anticancer activity as the interaction between these AMPs and DNA in cancer cells can cause DNA damage in cancer cells, blocking the division of cancer cells and resulting in cell death [7]. To have more insights on the antibacterial and anticancer mechanism of AMPs, studies on membrane bound structures and DNA binding ability of AMPs those are potent against both bacteria and cancer cells but not against normal mammalian cells are highly needed.

* Corresponding author. Address: School of Applied Sciences, Republic Polytechnic, 9 Woodlands Avenue 9, Singapore 738964, Singapore. Fax: +65 6779 2486.
E-mail address: chiradip_chatterjee@rp.sg (C. Chatterjee).

0006-291X/$ - see front matter © 2012 Elsevier Inc. All rights reserved.
http://dx.doi.org/10.1016/j.bbrc.2012.11.015

Lasioglossins, a new family of antimicrobial peptides, have strong antimicrobial activity with low haemo-lytic and mast cell degranulation activity, and exhibit cytotoxic activity against various cancer cells *in vitro*[8]. These pentadecapeptides are found in the venom of wild bees. The coupling constant $^{3}J_{NH,\alpha H}$ and chemical shifts of H_{α} protons data of Lasioglossins in trifluoroethanol/water indicated a curved α-helical conformation with a concave hydrophobic and convex hydrophilic side [8]. However there is no report on the detailed three dimensional structure of Lassioglossins in the presence of membrane mimetic micelles till date which is important to understand the mode of action of Lasioglossins for antimicrobial and anti cancer activity.

We have studied the interaction of Lasioglossin II (LL-II), one of the members of Lasioglossins family with membrane mimetic micelle, Dodecylphosphocholine (DPC) and plasmid DNA. We report here the fluorescence and CD spectroscopic studies on the interaction of LL-II with DPC micelle and the high-resolution NMR structure of LL-II complexed with DPC micelles. Moreover we have studied the DNA-binding property of this peptide by agarose gel retardation assay and fluorescence experiments.

2. Materials and methods

2.1. Materials

98% pure LL-II (H-Val-Asn-Trp-Lys-Lys-Ile-Leu-Gly-Lys-Ile-Ile-Lys-Val-Ala-Lys-NH_2) was purchased from GL Biochem (Shanghai) Ltd and used without further purifications. Sodium dodecyl sulfate (SDS) and DPC were obtained from Avanti Polar Lipids. Perdeuterated DPC-d_{38} was purchased from Cambridge Isotope Laboratories (CIL Inc). pUC19 plasmid DNA was purchased from Invitrogen and used without further purification. Ethidium bromide was purchased from Sigma. All other reagents and solvents were of reagent grade and used without further purification unless otherwise specified.

2.2. Fluorescence spectroscopy

Intrinsic fluorescence measurements were recorded using Perkin Elmer LS55 fluorescence spectrophotometers. Peptide fluorescence was measured by exciting peptide samples at 280 nm and scanning emission between 300 and 500 nm using a slit width of 3 nm at room temperature (~25 °C) and baseline corrected using proper control. After addition of the peptide, the system was equilibrated for 5 min before fluorescence was measured for every experiment.

2.3. CD spectroscopy

The secondary structure of LL-II in DPC micelle was recorded in a Jasco J810 spectropolarimeter (Jasco Corp., Tokyo, Japan) at room temperature (~25 °C) using 0.1 cm path length cuvette and baseline corrected using proper control. All samples were prepared in Millipore water (pH 4.3, adjusted with HCl) for recording the CD spectra in DPC micelle. The peptide concentration was maintained at 20 μM in all cases, and the concentration of the micelle was maintained well above the critical micelle concentration (CMC).

2.4. NMR spectroscopy

NMR measurements were performed on a Bruker Avance DRX800 operating at 800 MHz with cryo-probe and Bruker Avance DRX400 operating at 400 MHz. The sample temperature was maintained at 298 K. The samples were prepared with 2 mM peptide, 120 mM d_{38}- DPC (CIL, Cambridge, MA, USA) and 10% D_2O in Millipore water (pH 4.3 adjusted using dil HCl). 2D TOCSY spectra (spin-lock time of 100 ms) were acquired using the MLEV- 17 pulse sequence [9]. ^{1}H 2D NOESY spectra were acquired using a 150 ms mixing time [10]. Water suppression was achieved using the WATERGATE technique [11]. The NMR spectra were collected with 4096 and 512 data points in the direct and indirect dimensions, respectively, with 16 transients. The raw data were processed using TopSpin 2.1 (Bruker Scientific Inc), and resonance assignments were done using the Sparky [12].

To determine the sites of interaction between the peptide side chains and DPC, 2 mM LL-II in 9:1 H_2O/ D_2O was mixed with 50 mM protonated DPC [^{1}H DPC] micelles. Two-dimensional ^{1}H NOESY spectra were acquired at 298 K, with mixing times of 150 ms on a Bruker Avance DRX 800 MHz NMR spectrometer equipped with a cryo-probe. Spectra were acquired and processed as described above.

2.5. Structure calculation

The 3D structures of LL-II bound to DPC were calculated based on NOE derived distance constraints from 2D NOESY spectra and dihedral angle constrains obtained from TALOS [13]. Assignment of the proton spectra of Lassioglossin in the presence of membrane mimetic solvent (DPC) was accomplished using the technique of sequence-specific resonance assignments developed by Wüthrich [14]. On the basis of cross-peak intensities NOEs were qualitatively categorized to strong, medium and weak and then translated to upper bound distance limits to 2.5, 3.5 and 5.5 Å, respectively. The lower bounds for all NOE restraints were set to 2.0 Å. Initial structures were generated by backbone torsion angle restraints and distance geometry using CYANA-2.1 [13,14]. A total of 100 structures were calculated, and 20 lowest-energy structures with no distance violations greater than 0.2 Å or dihedral angle violations larger than 2 Å were selected. All the structures were analyzed using Pymol program (http://pymol.sourceforge.net).

2.6. DNA gel retardation assay

The pUC19 DNA was mixed with increasing amounts of peptides in 15 μl of 10 mM Tris, 50 mM NaCl, 1 mM EDTA buffer, pH 7.6 and the mixtures incubated at room temperature for 5 min, and subsequently subjected to electrophoresis on a 1% agarose gel in the TBE buffer.

3. Results and discussion

3.1. Interaction of LL-II with lipid micelles

3.1.1. Tryptophan fluorescence

The change in fluorescence intensity and the shift in maximum emission wavelength of tryptophan (Trp) fluorophore at the N-terminus of LL-II in the presence of SDS and DPC was examined which provides information about the environment of the Trp fluorophore. The maximum emission wavelength of LL-II in aqueous solution is 360 nm. A blue shift of approximately 27 nm was observed in the presence of SDS and DPC micelles (Fig. 1) indicating a significant interaction between the peptide and the hydrophobic core of the lipids.

The maximum fluorescence intensity of Trp in LL-II increased significantly in the presence of DPC micelles (Fig. 1) which indicates the insertion of the N-terminal tryptophan residue into the hydrophobic core of the lipid bilayer [15].

Although both the surfactants (SDS and DPC) promote a blue shift in the Trp fluorescence spectra, the fluorescence intensity was only increased significantly in DPC which indicates a more

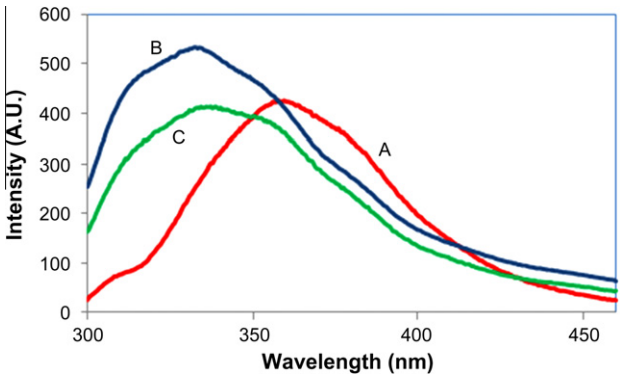

Fig. 1. Tryptophan (Trp) fluorescence emission spectra of LL-II (4 μM) (A) in buffer, (B) in the presence of 40 mM DPC and, (C) in the presence of 40 mM SDS micelles.

extensive partition to DPC and/or a more hydrophobic local micro environment for the tryptophan residue in DPC [15].

3.1.2. Circular Dichroism (Cd) analysis

The secondary structure of LL-II in the presence of DPC micelle was investigated by CD spectroscopy. In Millipore water (pH 4.3, adjusted with HCl) solution LL-II exhibits spectral characteristics of an unstructured peptide with a broad minimum at 198 nm (Fig. 2). The CD spectra underwent a considerable change in the presence of DPC micelle demonstrating a predominantly α-helical structure as indicated by the appearance of double minimum bands at 225 and 208 nm and positive CD band at 195 nm (Fig. 2). These data clearly indicate that LL-II interacts with DPC micelles undergoing conformational transitions from a prevalently random coil state to α-helical state. A similar α-helical structure formation was reported for LL-II in the anisotropic environment of the SDS micelles [8].

3.1.3. NMR structure of LL-II in the presence of d_{38}-DPC micelle

Čeřovsky et.al reported the coupling constant $^{3}J_{NH,\alpha H}$ and chemical shifts of H_α protons data of LL-II in water which were very close to the random coil values [8]. We have studied the structure of the LL-II in the presence of d_{38}-DPC micelles by 2D TOCSY and homonuclear NOESY spectroscopy. We assigned ~100%NOE peaks in the 2D TOCSY and NOESY spectrum and obtained 300 unambiguous NOEs. An ensemble of 100 structures for LL-II in DPC was calculated using Cyana-2.1 and best 20 structures were chosen for analysis. The complete chemical shift assignments of LL-II in presence of DPC micelle at 298 K is given in Supplementary Table 1.

Supplementary Fig. 1 shows that the difference in the chemical shift of peptide H_α *vs* random coil H_α is consistently negative almost throughout the peptide sequence in DPC micelles which suggests that the entire stretch of the peptide is helical or structured.

Supplementary Figs. 2 and 3 shows a summary of the backbone NOEs for the secondary structure assignment with a histogram indicating the number of NOEs per residue. We have detected several *d*NN ($i, i+1$) and *d*αN ($i, i+1$), as well as *d*NN($i, i+2$), throughout the entire peptide backbone. Also, several *d*αN ($i, i+3$) and *d*αN ($i, i+4$) NOE correlations diagnostic of α-helical conformation were detected from residues Val1 through Val13. While the highest density of NOE correlations was located between Asn2 and Leu7, there were a significant number of NOEs throughout the whole sequence of the peptide.

Structure calculations were based primarily on the NOESY spectra (Supplementary Figs. 4 and 5). The intra residue cross peaks are more intense from residue 2 to 14 (Supplementary Figs. 2 and 3) indicating the stretch of helical structure. Medium range NOE connectivities 11 dNN ($i, i+2$), 7 dαN ($i, i+2$), along with 7 dαN ($i, i+3$) and 5 dαN($i, i+4$) support the presence of 3–10-helix from residue 4 to 10. Presence of dαN ($i, i+4$) NOEs from residues Val1 to Lys12 suggests existence of some population of α-helix in this region. N-terminus is characterized by the presence of 7 dαN ($i, i+2$) NOEs. The propensity of half-turn seems to be more pronounced towards N-terminus as seen by the absence of dαβ ($i, i+3$) cross peaks. A summary of the constraints used for each residue is provided in Supplementary materials. The individual helical structure of LL-II spans from residues Val1 to Ala14 (Fig. 3A).

The superposition of the backbone atoms (Cα, C′ and N) of the 20 lowest energy structures of LL-II revealed that the peptide adopts a defined structure in DPC micelles (Fig. 3A and B). The structural statistics based on the 20 lowest energy structures for LL-II in DPC is shown in Table 1. The RMSD values are calculated for the well-structured helical portion of the peptide using MolMol viewing program [16]. The backbone pair wise RMSD values for all residues are 0.36 ± 0.20 Å and for all heavy atoms are 1.14 ± 0.40 Å. Moreover, the Ramachandran plot analysis using Procheck NMR [17] software tool showed that 83% of the residues were in favored or allowed regions and no residue is in disallowed region. The backbone dihedral angles (Φ, Ψ) were clustered mostly at the favored regions of the Ramachandran plot for all the residues in LL-II (Table 1).

Fig. 3C and D shows the surface diagram of LL-II bound to DPC micelle as well as charged and hydrophobic residues of the average structure of the peptide in lipid environment.

The hydrophobicity topography of LL-II clearly shows that the hydrophobic residues (Val1, Trp3, Val6, Leu7, Ile10, Val13, Ile11

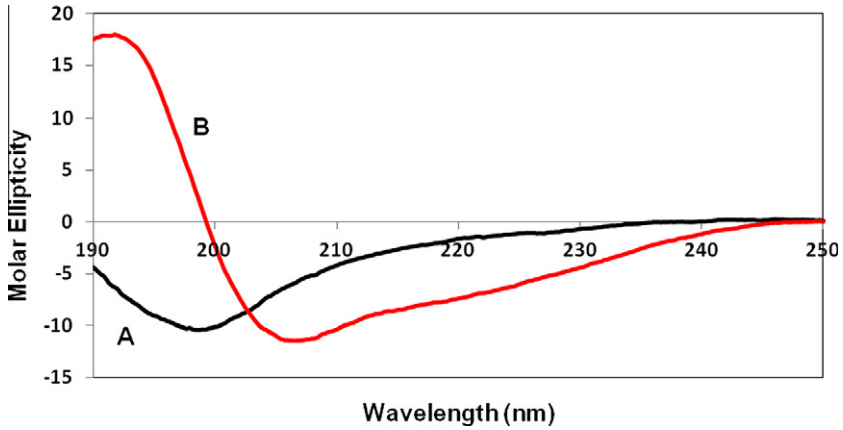

Fig. 2. Circular Dichroism spectra of the LL-II (A) in buffer and, (B) in the presence of 40 mM DPC micelle.

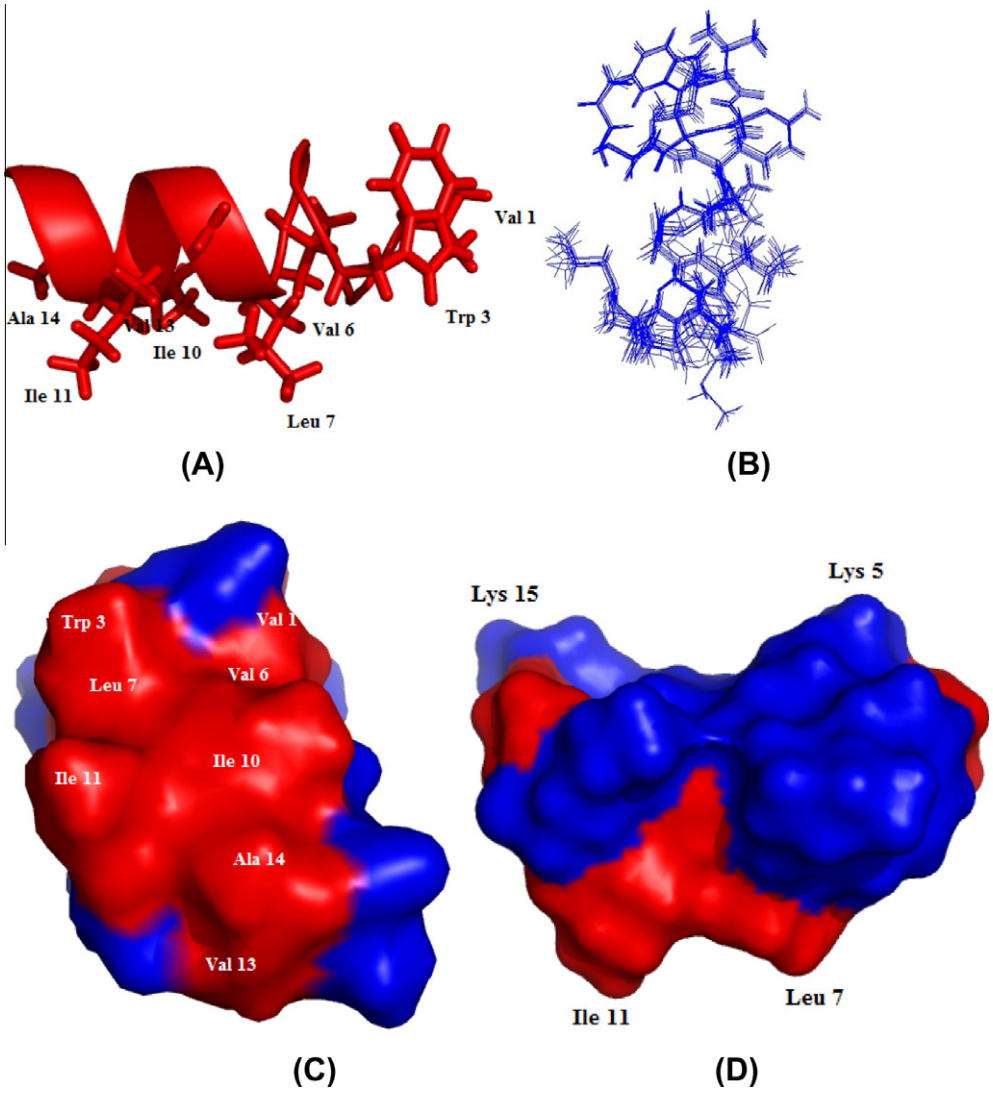

Fig. 3. (A) Ribbon representation of a representative monomeric helical structure of the LL-II in DPC micelle derived from structure calculation. The side chain of the amino acids is represented as sticks. (B) Superposition of backbone atoms of the twenty lowest energy structures of LL-II in DPC micelle. (C–D) Hydrophobicity topography for LL-II. The structures have the same relative orientation to each other. Red color denotes increasing hydrophobicity, while blue denotes hydrophilicity.(For interpretation of the references to color in this figure legend, the reader is referred to the web version of this article.).

and Ala14) cluster in one segment forming a hydrophobic patch. Val1 is found at the edge of a hydrophobic patch in LL-II. Trp3 at the N-terminus of LL-II is found to have its side chains protruding out which preferentially inserts into the lipid bilayer. Tryptophan residues have the unique ability to reside at the lipid water interface of a plasma membrane and the tryptophan fluorescence results demonstrate that the side chain of Trp3 interacts with lipid micelle. The hydrophobic side chain of Ile11 and Leu7 side chains likely inserts into the hydrophobic core of the membrane and both of these residues serve to anchor LL-II to the plasma membrane. The positively charged residues in the helical region, namely Lys4, Lys5, Lys9, Lys12 and Lys15 are oriented opposite to the hydrophobic patch due to which the helical portion of LL-II bound to DPC displays an amphipathic structure. From the structure of LL-II bound to DPC it can be suggested that the amphipathic α -helix of LL-II interacts with anionic membrane components *via* its basic amino acid residues. This type of binding mechanism is also found in cecropin B, an AMP with anticancer properties and derived from insects, where this binding mechanism mediates cytotoxic activity against cancer cells [5].

3.1.4. Intermolecular interaction between LL-II and protonated DPC micelle

The assignment of the DPC proton resonances was adapted from the published chemical shifts [18]. Quite a number of intermolecular NOEs between LL-II and DPC were observed, which clearly demonstrate complexation between LL-II and the micelles. NOE cross peaks observed between DPC (C2 and C4) protons with Asn2 and Trp3 groups of LL-II suggested possible N-terminal binding of the peptide with DPC micelle (Supplementary Fig. 6A and B). It should be noted that there were no NOE cross-peaks between the peptide and the buried terminal methyl group of protonated DPC (protons of C15). This confirms that the peptide does not pass through the micelle, but instead is localized to the surface of the micelle (Supplementary Fig. 8).

3.2. Interaction of LL-II with DNA

Since LL-II has been reported to act as an anti-cancer peptide [8], the interaction of LL-II with DNA was evaluated by Gel retardation assay and fluorescence quenching experiments. Using similar

Table 1
NMR statistics for the twenty lowest energy structures of LL-II bound to DPC micelle.

NOE distance constraints	
Intra residue (i−j) = 0	300
Sequential (|i−j| = 1)	101
Medium range (2 ⩽ |i−j| ⩾ 4)	190
Long range	9
Angle constraints	
Φ	10
Ψ	11
Distance restraints violations	
No. of violations (⩾0.25 Å)	0
Distance restraints violations	
No. of violations (⩾2 Å)	0
Deviation from mean structure	
Backbone RMSD (N, Cα, C′) (Å)	0.36 ± 0.20
Heavy atoms (Å)	1.14 ± 0.40
Ramachandran plot analysis (%)	
Most favored and allowed region	83
Generously allowed region	17
Disallowed region	0

experiments several DNA peptide interactions has been previously reported [6,19].

Different amount of peptide was mixed with a fixed amount (0.5 μg) of pUC19 plasmid DNA at a peptide/DNA weight ratio 0, 1, 2, 4, 6, 8, 10, 20, 30 and the complexes were electrophoresed on a 1% agarose gel (Fig. 4). At a peptide/DNA weight ratio of two, a fraction of the plasmid DNA was still able to migrate into the gel in the same way as non-complexed DNA, whereas, at a weight ratio of four, a significant retardation of the DNA was observed which increases with increasing amount of peptide showing that the DNA was aggregated by LL-II. The observation of DNA binding of LL-II is of interest for anti cancer activity of Lassioglosins peptide family. The peptide – membrane interaction represents the initial step of penetrating cell wall to reach the inner structure of the cell followed by the interaction of peptide with intercellular target like DNA which might play a part in the overall anticancer activity. The binding mode of the peptide with DNA was further supported by the fluorescence experiments, which might illustrate its anticancer mechanism.

To examine whether the DNA binding imparts conformational changes in LL-II peptide, quenching of the intrinsic tryptophan fluorescence of LL-II on addition of pUC19 DNA was studied. The intensity and the emission maximum of tryptophan fluorescence spectra changes when different conformations are observed on the surroundings of the indole ring of the tryptophan under different environment [19]. As shown in Supplementary Fig. 7, LL-II exhibited a fluorescence emission maximum at 360 nm in the absence of pUC19 DNA. Addition of DNA caused the fluorescence intensity to decrease and the emission maximum to shift from 361 to 359 nm, showing that conformational changes occurred in the environment of tryptophan residues on DNA binding which also provides evidence of direct interaction of DNA and the Trp residue of the peptide.

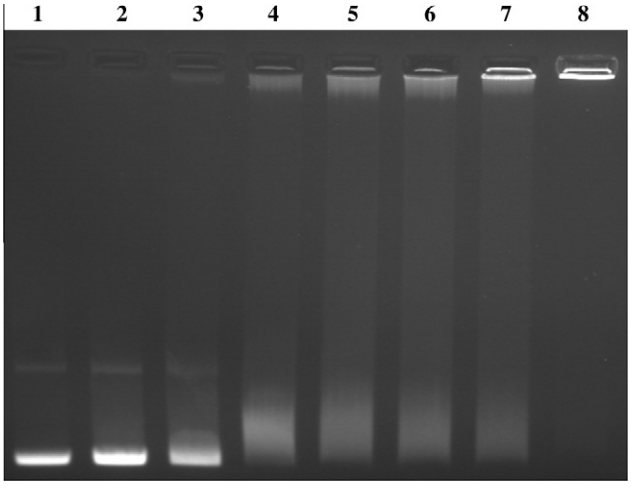

Fig. 4. Gel retardation analysis of the binding of LL-II to pUC19 DNA. Band 1, free DNA (0.5 μgm); and Bands 2–8, DNA with increasing amounts of LL-II (0.5, 1, 2, 3, 4, 5, 10, 15 μgm).

In summary we have provided the evidences for the interaction of the N-terminal tryptophan residue of LL-II with the hydrophobic core of DPC micelles, and reported the first NMR structure of LL-II complexed with DPC micelles. This structure indicates that LL-II adopts an ampipathic α -helical conformation in the presence of DPC micelles where the hydrophobic residues cluster in one segment forming a hydrophobic patch and the positively charged residues are oriented opposite to the hydrophobic patch. The ability of LL-II to form a well defined ampipathic α -helix in the presence of DPC micelles is responsible for high antimicrobial and low hemolytic activity of LL-II. Moreover the gel retardation and fluorescence quenching experiments confirmed the DNA-binding ability of LL-II which may mediate cytotoxic activity of LL-II against various cancer cells *in vitro*. Knowledge of the micelle bound structures and DNA binding ability of LL-II will lead to understand the mechanism of action of the anti cancer activity of this antimicrobial peptide.

Acknowledgments

The authors would like to thank the NMR facility School of Applied Sciences, Republic Polytechnic and NMR facility, Department of Biological Sciences, National University of Singapore. Help from Mr. Manjeet Mukherjee, graduate student, NUS is greatly appreciated. The atomic coordinates and NMR constrains of membrane bound LL-II structure are deposited to BioMag-ResBank (BMRB) under the accession code 21017.

Appendix A. Supplementary data

Supplementary data associated with this article can be found, in the online version, at http://dx.doi.org/10.1016/j.bbrc.2012.11.015.

References

[1] M. Zasloff, Antimicrobial peptides of multicellular organisms, Nature 415 (2002) 389–395.
[2] M. Zasloff, Antibiotic peptides as mediators of innate immunity, Curr. Opin. Immunol. 4 (2000) 3–7.
[3] R.E. Hancock, G. Diamond, The role of cationic antimicrobial peptides in innate host defences, Trends Microbiol. 8 (2000) 402–410.
[4] Y. Rosenfeld, Y. Shai, Lipopolysaccharide (Endotoxin)-host defense antibacterial peptides interactions: role in bacterial resistance and prevention of sepsis, BBA-Biomembranes 1758 (2006) 1513–1522.
[5] D.W. Hoskin, A. Ramamoorthy, Studies on anticancer activities of antimicrobial peptides, Biochim. Biophys. Acta 1778 (2) (2008) 357–375.
[6] Y.L. Tang, Y.H. Shi, W. Zhao, et al., Interaction of MDpep9, a novel antimicrobial peptide from Chinese traditional edible larvae of housefly, with Escherichia coli genomic DNA, Food Chem. 115 (2009) 867–872.
[7] A. Mor, Peptide-based antibiotics: a potential answer to raging antimicrobial resistance, Drug Dev. Res. 50 (2000) 440–447.
[8] V. Čeřovsky, M. Budesnsk, O. Hovorka, et al., Lasioglossins: three novel antimicrobial peptides from the venom of the eusocial bee lasioglossum laticeps (hymenoptera: halictidae), ChemBioChem 10 (2009) 2089–2099.
[9] A. Bax, D.G. Davis, MLEV-17 based two-dimensional homonuclear magnetization transfer spectroscopy, J. Magn. Reson. 65 (1985) 355–360.
[10] A. Kumar, R.R. Ernst, K. Wuthrich, A Two-Dimensional Nuclear Overhauser Enhancement (2D NOESY) experiment for the elucidation of complete proton–proton cross relaxation networks in biological macromolecules, Biochem. Biophys. Res. Commun. 95 (1980) 1–6.

[11] M. Piotto, V. Saudek, V. Skelnar, Gradient-Tailored excitation for single-quantum nmr spectroscopy of aqueous solution, J. Biomol. NMR. 2 (1992) 661–665.

[12] T.D. Goddard, D.G. Kneller, Sparky 3, University of California, San Francisco.

[13] T. Herrmann, P. Guntert, K. Wuthrich, Protein NMR structure determination with automated NOE assignment using the new software CANDID and the torsion angle dynamics algorithm DYANA, J. Mol. Biol. 319 (2002) 209–227.

[14] K. Wüthrich, NMR of Proteins and Nucleic Acids, J. Wiley & Sons, New York, 1986.

[15] E.F. Haney, F. Lau, H.J. Vogel, Solution structures and model membrane interactions of lactoferrampin, an antimicrobial peptide derived from bovine lactoferrin, Biochim. Biophys. Acta 1768 (2007) 2355–2364.

[16] R. Koradi, M. Billeter, K. Wuthrich, MOLMOL: a program for display and analysis of macromolecular structures, J. Mol. Graphics 14 (1996) 51–55.

[17] R.A. Laskowski, J.A. Rullmannn, M.W. MacArthur, et al., AQUA and PROCHECK-NMR: programs for checking the quality of protein structures solved by NMR, J. Biomol. NMR 8 (1996) 477–486.

[18] H.W. Van Den Hooven, C.A.E.M. Spronk, M. Van De Kamp, et al., Surface location and orientation of the lantibiotic nisin bound to membrane-mimicking micelles of dodecylphosphocholine and of sodium dodecylsulphate, Eur. J. Biochem. 235 (1996) 394–403.

[19] H. Chun-Hua, C. Chinpan, J. Maou-Lin, et al., Structural and DNA-binding studies on the bovine antimicrobial peptide, indolicidin: evidence for multiple conformations involved in binding to membranes and DNA, Nucleic Acids Res. 33 (2005) 4053–4064.